CHARACTERISTICS OF PEO-dibutyltin bis{p-[N-(3,4-dinitro phenyl)] amino benzoate}and PEO-dioctyltin bis{p-[N-(3,4-dinitro phenyl)] amino benzoate}

4.1 Introduction

Different concentrations (Sn/EO=0.015, 0.031, 0.063, 0.125) of the PEO-dibutyltin bis{p-[N-(3,4-dinitro phenyl)]amino benzoate} and PEO- dioctyltin bis{p-[N-(3,4-dinitro phenyl)]amino benzoate} polymer electrolyte films were prepared using the technique as mentioned in section 2.1.2. As discussed earlier in section 3.1 small quantities of propylene carbonate (PC) and ethylene carbonate (EC) were added in order to enhance the conductivity. The composition that afforded the best conductivity for PEO-dibutyltin bis{p-[N-(3,4-dinitro phenyl)]amino benzoate}: EC: PC and PEO-dioctyltin bis{p-[N-(3,4-dinitro phenyl)]amino benzoate} is 85:13:2. These electrolytes were hence used for the cell fabrication and discharge characteristics.

4.2 UV – Visible Spectral Analysis

UV-Visible spectra of pure PEO film, PEO-doped dibutyltin bis{p-[N-(3,4-dinitro phenyl)]amino benzoate} film and pure dibutyltin bis{p-[N-(3,4-dinitro phenyl)]amino benzoate} powder in acetonitrile are depicted in Figure 4.1. For purposes of comparision, the spectrum of pure dibutyltin bis{p-[N-(3,4-dinitro phenyl)]amino benzoate} was recorded at two different concentrations in acetonitrile as shown in Figure 4.2. It is seen that the absorption spectra of the dibutyltin bis{p-[N-(3,4-dinitro phenyl)]amino

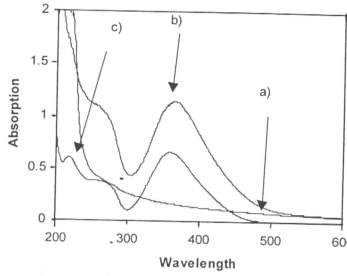

Figure 4.1: UV-Visible spectrum for a)pure PEO b) PEO - dibutyltin bis{p-[N-(3,4-dinitro phenyl)]amino benzoate} and c) dibutyltin bis{p-[N-(3,4-dinitro phenyl)]amino benzoate} in acetonotrile.

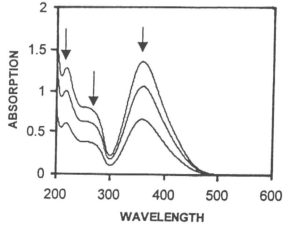

Figure 4.2: UV-Visible absorption spectrum for dibutyltin bis{p-[N-(3,4-dinitro phenyl)]amino benzoate} in acetonitrile at different concentrations.

benzoate} are essentially unchanged at the two concentrations and both reveal characteristic bands at 220nm and 365nm, along with a weak shoulder at 254nm.

In the PEO-doped polymer film, the band at 365nm is shifted to 354nm and the shoulder at 254nm to 260nm. No peak is observed at 220nm. These shifts are taken as evidence of the presence of the organotin in the PEO matrix.

4.3 IR - Spectral Analysis

The IR spectra of pure PEO (Figure 3.3), pure dibutyltin bis{p-[N-(3,4-dinitro phenyl)]amino benzoate}, pure dioctyltin bis{p-[N-(3,4-dinitro phenyl)]amino benzoate}, PEO-dibutyltin bis {p-[N-(3,4-dinitro phenyl)]amino benzoate} and PEO-dioctyltin bis{p-[N-(3,4-dinitro phenyl)]amino benzoate} are compared in Figures 4.3 to 4.6, respectively. In the case of PEO-dibutyltin bis{p-[N-(3,4-dinitro phenyl)]amino benzoate} significant bands were observed at 774, 741, 706, 641, and 593 cm^{-1} as seen in Figure 4.4. These bands are characteristic of dibutyltin bis {p-[N-(3,4-dinitro phenyl)]amino benzoate} as seen in Figure 4.3 . Although the bands in Figure 4.4 at 774, 741 and 706 cm^{-1} appear at the same positions as in Figure 4.3, the bands at 641 and 593 cm^{-1} shows slight shifts in their positions. Similarly the IR spectrum of PEO-dioctyltin bis {p-[N-(3,4-dinitro phenyl)]amino benzoate} shows bands at 767, 734, 700 and 654cm^{-1} (Figure 4.6). These bands are characteristic bands of dioctyltin bis{p-[N-(3,4-dinitro phenyl)]amino benzoate} appearing with

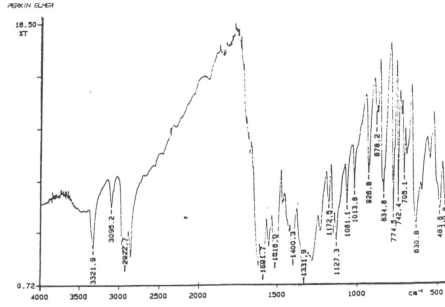

Figure 4.3: Infrared spectrum of pure dibutyltin bis{p-[N-(3,4-dinitro phenyl)]amino benzoate.

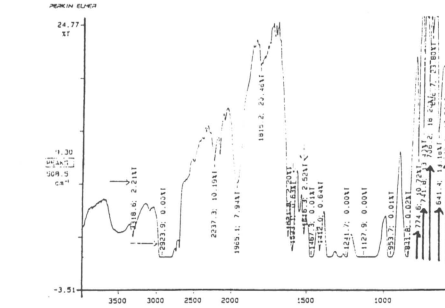

Figure 4.4: Infrared spectrum of PEO - dibutyltin bis{p-[N-(3,4-dinitro phenyl)]amino benzoate}

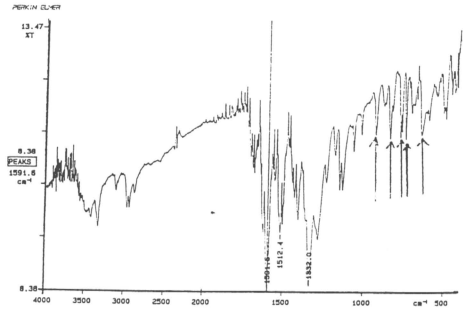

Figure 4.5: Infrared spectrum of pure dioctyltin bis{p-[N-(3,4-dinitrophenyl)]amino benzoate}

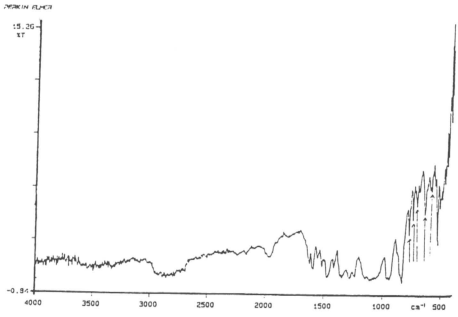

Figure 4.6: Infrared spectrum of PEO-dioctyltin bis{p-[N-(3,4-dinitro phenyl)]amino benzoate}

slight shift in the peak positions. These slight shifts in the band positions may be indicative of complex formation between PEO and respective diorganotin dopants.

4.4 XRD Analysis

The X - ray diffraction patterns of PEO , PEO - dibutyltin bis{p-[N-(3,4-dinitro phenyl)]amino benzoate} and PEO - dioctyltin bis{p-[N-(3,4-dinitro phenyl)]amino benzoate} systems are as shown in Figures 4.7, 4.8 and 4.9. Sharp and intense peaks occur at $2\theta = 20^0$ and 24^0 , in the range $10 - 70^0$ for the case of undoped PEO (Fig.4.7) are indicative of some degree of crystallinity in the polymer. These peaks, although still present in the diorganotin-doped PEO, show slight shifts in their position and strong reduction in relative intensity.

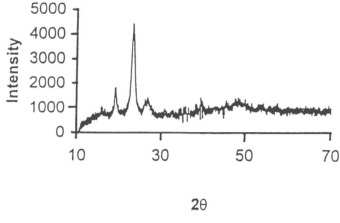

Figure 4.7: X - ray diffractogram for pure PEO

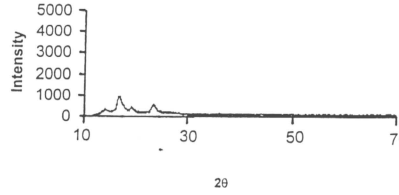

Figure 4.8: X - ray diffractogram for PEO - dibutyltin bis{p-[N-(3,4-dinitro phenyl)]amino benzoate (Sn/EO = 0.031).

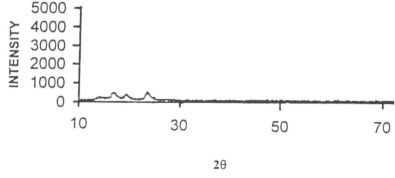

Figure 4.9: X - ray diffractogram for PEO-dioctyltin bis{p-[N-(3,4-dinitro phenyl)]amino benzoate} (Sn/EO = 0.031).

This suggests that the added organotin intruding into the crystalline regions of the polymer cause the transformation of these regions to the amorphous state, in conformity with observations on other PEO- systems doped with inorganic salts at below saturation levels [38,40]. This probably accounts for the higher conductivity values for PEO doped dibutyltin bis{p-[N-(3,4-dinitro phenyl)]amino benzoate} and PEO doped dioctyltin bis{p-[N-(3,4-dinitro phenyl)]amino benzoate} relative to undoped PEO (*vide infra*).

4.5 Impedance Spectroscopy Analysis

It is necessary to know the electrical conductivity of the samples so that the sample with composition giving the highest electrical conductivity can be identified and used for the fabrication of electrochemical cells.

4.5.1 Room Temperature Dependence of Electrical Conductivity

From the data of Impedance spectroscopy, the Cole - Cole plot is constructed by plotting the imaginary impedance magnitude ($Z_i = Z \sin\theta$) against the real impedance magnitude ($Z_r = Z \cos\theta$) . The Cole – Cole plots obtained on films of different compositions of PEO-dibutyltin bis{p-[N-(3,4-dinitro phenyl)]amino benzoate} and PEO-dioctyltin bis{p-[N-(3,4-dinitro phenyl)]amino benzoate} are depicted in Figures 4.10 (a - e) and 4.11(a - e). The electrical conductivity was calculated as explained in chapter 3 (section 3.6.1); the values are tabulated in Table 4.1.

From the data it can be seen that the conductivity of the PEO-dibutyltin bis{p-[N-(3,4-dinitro phenyl)]amino benzoate} and PEO- dioctyltin

bis{p-[N-(3,4-dinitro phenyl)]amino benzoate}systems vary with the Sn/EO ratio . This trend is illustrated in Figures 4.12 and 4.13.

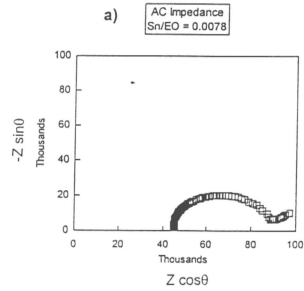

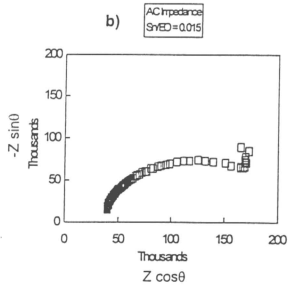

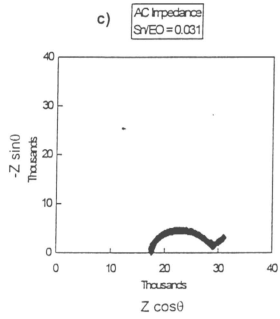
c)
AC Impedance
SnVEO = 0.031
-Z sin()
Thousands
Thousands
Z cosθ

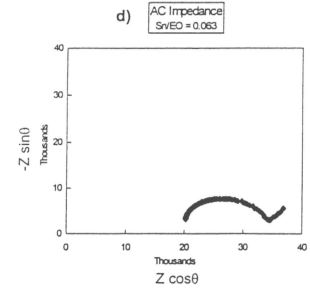
d)
AC Impedance
SnVEO = 0.063
-Z sin()
Thousands
Thousands
Z cosθ

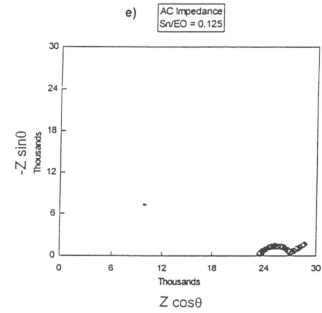

Figure 4.10 : Cole – Cole plots (a - e) for different compositions of PEO- dibutyltin bis{p-[N-(3,4-dinitro phenyl)]amino benzoate} system.

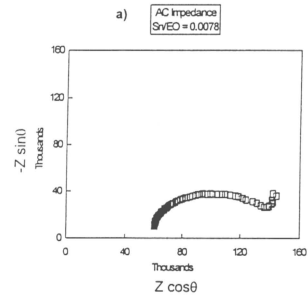

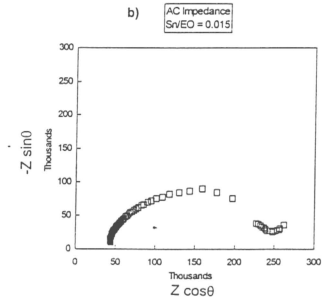
b)
AC Impedance
Sn/EO = 0.015
300
250
200
150
100
50
0
-Z sinθ
Thousands
0
50
100
150
200
250
300
Thousands
Z cosθ

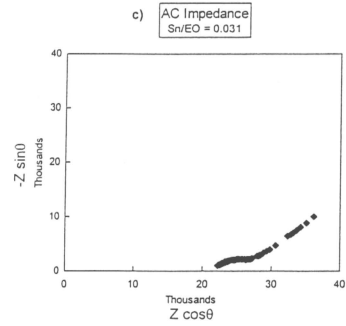
c)
AC Impedance
Sn/EO = 0.031
40
30
20
10
0
-Z sinθ
Thousands
0
10
20
30
40
Thousands
Z cosθ

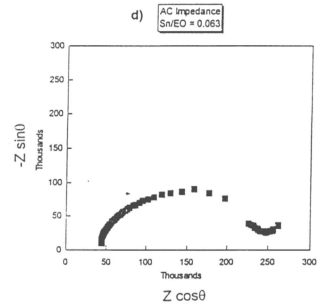

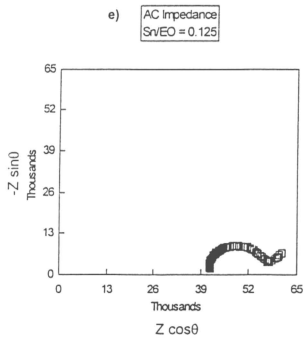

Figure 4.11: Cole - Cole plots (a - e) for PEO- dioctyltin bis{p-[N-(3,4-dinitro phenyl)]amino benzoate} system.

Table 4.1: Ionic conductivity values from the Cole-Cole plots of PEO-dibutyltin bis{p-[N-(3,4-dinitro phenyl)]amino benzoate} and PEO- dioctyltin bis{p-[N-(3,4-dinitro phenyl)]amino benzoate.

PEO-dibutyltin

Mole ratio of Sn/EO	Conductivity S/cm
0	4×10^{-9}
0.0078	1.68×10^{-7}
0.015	1.88×10^{-7}
0.031	4.36×10^{-7}
0.063	3.34×10^{-7}
0.125	2.88×10^{-7}

PEO-dioctyltin

Mole ratio of Sn/EO	Conductivity S/cm
0	4×10^{-9}
0.0078	1.43×10^{-7}
0.015	1.69×10^{-7}
0.031	3.46×10^{-7}
0.063	1.89×10^{-7}
0.125	1.62×10^{-7}

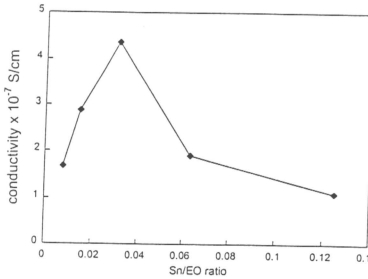

Figure 4.12: Compositional dependence of conductivity of PEO-dibutyltin bis{p-[N-(3,4-dinitro phenyl)]amino benzoate}

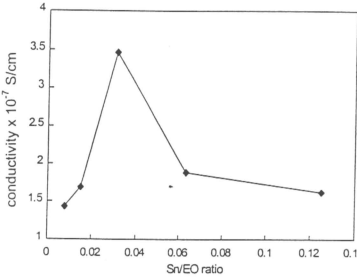

Figure 4.13: Compositional dependence of conductivity of PEO-dioctyltin bis{p-[N-(3,4-dinitro phenyl)]amino benzoate}

With an increase in the Sn/EO ratio, the conductivity reaches a maximum of 4.36 x 10^{-7} S/cm for PEO-dibutyltin bis{p-[N-(3,4-dinitro phenyl)]amino benzoate} and 3.46 x 10^{-7} S/cm for PEO - dioctyltin bis{p-[N-(3,4-dinitro phenyl)]amino benzoate} at Sn/EO = 0.031. In PEO electrolytes, it is generally accepted that the conduction phases are amorphous phases containing these dopants [87]. Therefore, the initial rise in conductivity can be attributed to the increase in the number of charge carriers and also to the decrease in crystallinity of the system with increasing salt concentration [88]. On the other hand, the decrease in the conductivity of PEO-dibutyltin bis{p-[N-(3,4-dinitro phenyl)]amino benzoate} and PEO-dioctyltin bis{p-[N-(3,4-dinitro phenyl)]amino benzoate} electrolytes observed at higher dopant concentrations can be related to the decrease

in ionic mobility [89] as well to the increase in the degree of crystallinity of PEO. The decrease in mobility is related to the increase in viscosity of the polymers on addition of dopants [90-92].

As these polymer electrolytes cannot be used as electrolytes for all solid state batteries at ambient temperature for the reasons already stated in Chapter 3, the plasticizers (EC & PC) were therefore added to the polymer electrolytes at different ratios to secure the best conducting samples. These were obtained for the composition (PEO-dibutyltin bis{p-[N-(3,4-dinitro phenyl)]amino benzoate}: EC: PC) 85:13:2 and (PEO-dioctyltin bis{p-[N-(3,4-dinitro phenyl)]amino benzoate} : EC: PC) 85:13:2 (see table 4.2).

4.5.2 Temperature Dependence of Electrical Conductivity (σ)

The temperature dependence of the electrical conductivity of PEO-dibutyltin bis{p-[N-(3,4-dinitro phenyl)]amino benzoate} and PEO-dioctyltin bis{p-[N-(3,4-dinitro phenyl)]amino benzoate} is shown in the data of Tables 4.3 and 4.4.

Table 4.2: Conductivity values of different compositions of PEO - dibutyltin bis{p-[N-(3,4-dinitro phenyl)]amino benzoate} : EC : PC and PEO - dioctyltin bis{p-[N-(3,4-dinitro phenyl)]amino benzoate}:EC: PC

PEO-dibutyltin : EC : PC

Sample composition	Electrical conductivity (S/cm)
85:13:2	2.25×10^{-6}
85:10:5	1.18×10^{-6}
85:8:7	0.95×10^{-6}

PEO-dioctyltin : EC:PC

Sample composition	Electrical conductivity (S/cm)
85:13:2	2.1×10^{-5}
85:10:5	1.4×10^{-6}
85:8:7	1.06×10^{-6}

The σ-T plots, given in Figures 4.14 and 4.15, are based on the data in Tables 4.3 and 4.4. Tables 4.5 and 4.6 show the variation of the activation energy values (E_A) (obtained from the ln (σT) versus $10^3/T$ plots of Figures 4.14 and 4.15) with Sn/EO composition.

Interestingly, the E_A values obtained in this study are almost identical to the values reported for other PEO-doped systems [74, 80]. The increase in conductivity is attributed to the decrease in E_A while the decrease in conductivity after the Sn/EO = 0.031 ratio is attributed to the ions needing much more energy to begin motion.

Table 4.3: Data for the generation of (ln (σT) Vs 1/T) plots for PEO - dibutyltin bis{p-[N-(3,4-dinitro phenyl)]amino benzoate}

$10^3/T$	ln (σT) values for different compositions of Sn/EO					
(K^{-1})	0	0.0078	0.015	0.031	0.063	0.125
3.3	-13.62	-9.89	-9.35	-8.93 (-7.29)	-9.76	-10.3
3.2	-13.22	-9.5	-9.01	-8.62 (-7.03)	-9.43	-9.93
3.1	-12.80	-9.11	-8.66	-8.32 (-6.77)	-9.1	-9.56
3.05	-12.60	-8.92	-8.49	-8.17 (-6.64)	-8.94	-9.38
3.0	-12.41	-8.72	-8.31	-8.02 (-6.51)	-8.77	-9.17
2.95	-12.20	-8.52	-8.14	-7.87 (-6.38)	-8.61	-8.99
2.9	-11.98	-8.33	-7.96	-7.7 (-6.25)	-8.44	-8.82
2.8	-10.58	-6.79	-6.54	-6.14 (-5.09)	-6.99	-7.35
2.7	-9.82	-6.04	-5.92	-5.72 (-4.53)	-6.35	-6.71

- Data in parentheses are for the composition with added EC/PC i.e PEO-dibutyltin:EC:PC (85:13:2)

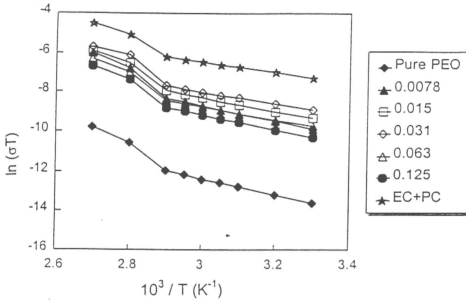

Figure 4.14: Arrhenius plots for different compositions of PEO-dibutyltin bis{p-[N-(3,4-dinitro phenyl)]amino benzoate} system

Table4.4: Data for the generation of (ln (σT) Vs 1/T) plots for PEO - dioctyltin bis{p-[N-(3,4-dinitro phenyl)]amino benzoate}

10^3/T	ln (σT) values for different compositions of Sn/EO					
(K^{-1})	0	0.0078	0.015	0.031	0.063	0.125
3.3	-13.62	-10.04	-9.87	-9.16 (-7.36)	-9.76	-9.92
3.2	-13.22	-9.66	-9.51	-8.84 (-7.08)	-9.41	-9.57
3.1	-12.80	-9.28	-9.15	-8.52(-6.80)	-9.06	-9.23
3.05	-12.6	-9.19	-8.97	-8.36(-6.66)	-8.89	-9.06
3.0	-12.41	-8.9	-8.78	-8.2(-6.52)	-8.69	-8.87
2.95	-12.2	-8.71	-8.6	-8.04(-6.38)	-8.52	-8.6
2.9	-11.98	-8.53	-8.44	-7.86(-6.24)	-8.36	-8.52
2.8	-10.58	-7.15	-7.07	-6.54(-4.96)	-6.79	-6.57
2.7	-9.82	-6.75	-6.71	-6.06(-4.18)	-6.16	-5.82

- Data in parentheses are for the composition with added EC/PC i.e PEO-dioctyltin:EC:PC (85:13:2)

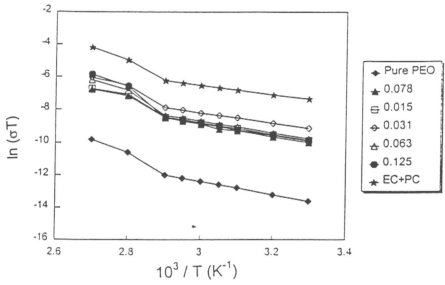

Figure 4.15: Arrhenius plots of various concentrations in the PEO-dioctyltin bis{p-[N-(3,4-dinitro phenyl)]amino benzoate} system.

Table 4.5: Activation energy values, E_A, for PEO-dibutyltin

Composition of Sn/EO	Gradient ($-E_A/k$)	E_A (eV)
0	4000	0.344
0.0078	3900	0.335
0.015	3400	0.292
0.031	3100	0.266
0.063	3300	0.283
0.125	3700	0.318

Table 4.6: Activation energy values, E_A, for PEO-dioctyltin

Composition of Sn/EO	Gradient ($-E_A/k$)	E_A (eV)
0	4000	0.344
0.0078	3800	0.327
0.015	3600	0.309
0.031	3200	0.275
0.063	3500	0.301
0.125	3550	0.305

Since conductivity is related to the number of carrier ions as well as their mobility, it can be concluded that the conductivity is influenced by many factors such as incorporated impurities, degree of crystallinity and morphological structure of polymer – dopant systems . Therefore to have a better understanding and to seek further evidence for what has been stated above, it is necessary to carry out SEM-EDAX analysis on the as-

prepared polymer electrolyte films.

4.6 SEM –EDAX Analysis

Figures 4.16 & 4.17 illustrate the SEM micrographs of films of PEO-dibutyltin bis{p-[N-(3,4-dinitro phenyl)]amino benzoate}:EC:PC and PEO-dioctyltin bis{p-[N-(3,4-dinitro phenyl)]amino benzoate}:EC:PC.

As discussed in Chapter 3 (Section 3.7) the disappearance of the spherulitic regions in Figures 4.16 & 4.17 when compared with the micrograph of pure PEO suggests that the doped polymers are essentially amorphous. With the reduction in crystallinity, the electrical conductivity increases as borne out by the ac impedance studies.

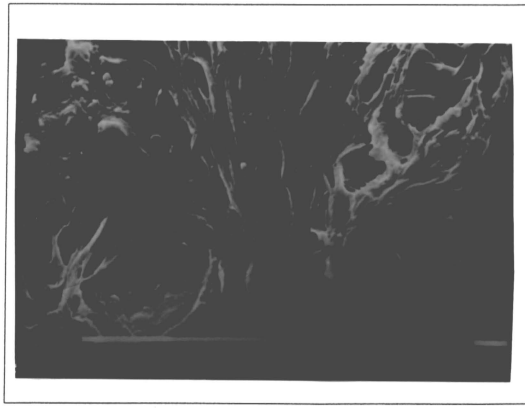

Figure 4.16 : SEM micrograph of PEO-dibutyltin bis{p-[N-(3,4-dinitro phenyl)]amino benzoate}:EC:PC

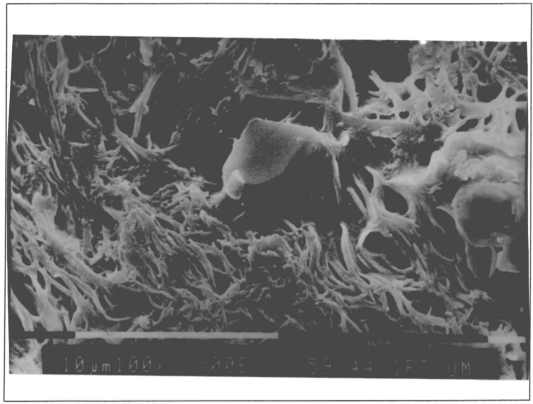

Figure4.17: SEM micrograph of PEO-dioctyltin bis{p-[N-(3,4-dinitro phenyl)]amino benzoate}:EC:PC

Figures 4.18 & 4.19 show the EDAX pictures obtained upon analysing the samples of PEO- dibutyltin bis{p-[N-(3,4-dinitro phenyl)]amino benzoate} (32:1) film and PEO-dioctyltin bis{p-[N-(3,4-dinitro phenyl)]amino benzoate} (32:1) film. The peaks attributable to Sn and Cl are clearly in evidence and attest unequivocally to the presence of dibuytltin and dioctyltin dopants in the polymer matrix.

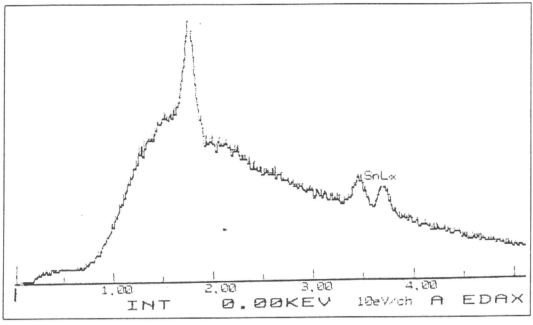

Figure 4.18: EDAX data for PEO- PEO-dibutyltin bis{p-[N-(3,4-dinitro phenyl)]amino benzoate}:EC:PC

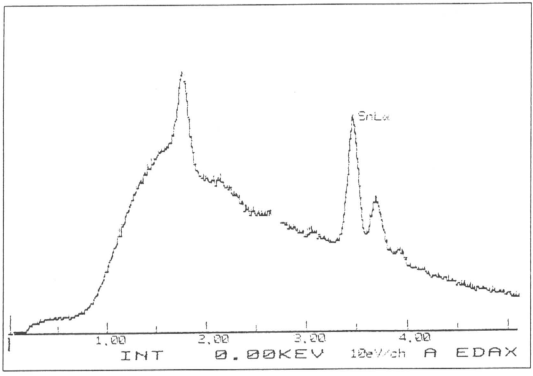

Figure 4.19: EDAX data for PEO - dioctyltin bis{p-[N-(3,4-dinitro phenyl)]amino benzoate}:EC:PC

4.7 Electrochemical Cell Characterization

Films of PEO- dibutyltin bis{p-[N-(3,4-dinitro phenyl)]amino benzoate}: EC: PC and PEO- dioctyltin bis{p-[N-(3,4-dinitro phenyl)]amino benzoate} with composition 85:13:2 which showed the highest electrical conductivity in tests using impedance spectroscopy were used as the electrolyte component in the electrochemical cell fabrication. The anode consisted of Sn metal foil while the cathode consisted of intercalated composite cathode of MnO_2 deposited as a film on copper mesh as described in section 2.1.3. The anode, electrolyte and the cathode were then clamped between two glass plates and then connected via the electrodes to a computer-controlled galvanostat (BAS LG – 50) for characterization and discharge characteristics.

The open circuit voltage is the voltage of the cell when there is no current flow through the external circuit. It is different from the potential difference (P.D) of the cell i.e the voltage of the cell when a certain current has been drawn out of it. Table 4.7 gives the values of OCV for each fabricated cell. These voltages are the result of the half-cell reactions between the anode and the cathode species at equilibrium via which the ions travel through the solid electrolytes of PEO - dibutyltin bis{p-[N(3,4-dinitrophenyl)]amino benzoate} system and PEO-dioctyltin bis{p-[N-(3,4-dinitro phenyl)]amino benzoate} system.

Figures 4.20 (a&b) show the discharge characteristics for the fabricated cells at a constant load current of 10μA. It is found that the voltage of the cell drops at the beginning of the discharge and as the

discharge proceeds the voltage seems to be quite stable for many minutes in the plateau region before it decreases again.

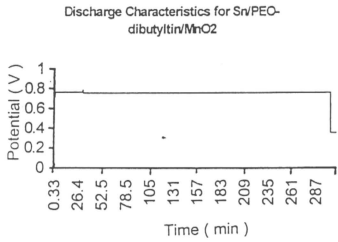

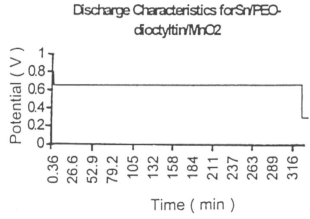

Figure 4.20 : Discharge curves for the fabricated cells.

Table 4.7: Open circuit voltage for the fabricated cells.

SAMPLE COMPOSITION	OCV
Sn/PEO-dibutyltin:EC:PC/MnO_2	0.85 V
Sn/PEO-dioctyltin:EC:PC/MnO_2	0.8 V

Discharge curves such as depicted in Figure 4.20 (a&b) are useful, in that they allow estimation of the cell capacity, based on the relation, Cell capacity = Discharge current associated with the plateau region x Time span of the plateau. The cell capacity thus obtained are tabulated in Table 4.8.

Table 4.8: Cell capacity of fabricated cells

SAMPLE COMPOSITION	CELL CAPACITY(mA-h)
Sn/PEO-dibutyltin:EC:PC/MnO_2	0.04
Sn/PEO-dioctyltin:EC:PC/MnO_2	0.05

As mentioned in Chapter3 (Section 3.8) the theoretical OCV value of the above cells is also 1.36V, since this is determined only by the value of the electrodes and not by the electrolyte medium. The experimentally obtained OCV values are 60% - 70% of the theoretical value.